韓國海洋工學會誌 第12卷 第1號, pp.85~98, 1998. 2

◉ 論 文

A Numerical Study of Nonlinear Free-Surface Flows Generated by Motions of Two Dimensional Cylinders

Ho-Young Lee*

(97년 5월 26일 접수)

2차원 실린더의 운동에 기인한 비선형 자유표면 유동의 수치해석

이 호 영*

Key Words : Cauchy's Theorem, Fully Nonlinear Free Surface, Matching Condition, Two-Dimensional Transient Green Function, Nonlinear Domain, Linear Domain

초 록

본 논문의 수치해법은 경계치문제를 풀기 위하여 코시이론(Cauchy's theorem)을 사용하였다. 경계치문제는 완전한 물체표면조건과 자유표면 조건을 만족시키는 초기치문제로 귀결된다. 현 수치해법에서 무한영역은 수치계산 영역인 비선형 영역과 선형 자유표면 조건을 만족하는 선형 영역으로 나누어 진다. 선형영역의 해는 과도 그린(Green)함수를 사용하여 정합조건을 부과함으로써, 수치계산은 비선형 영역에서만 수행된다. 본 논문에서 저자는 수치계산 영역에서 코시이론을 사용하여 적분방정식을 도출하였고, 무한영역의 해는 정합면에서 과도 그린함수를 사용하여 표현하였다. 본 수치계산에서 자유표면에 요소 재분배법을 적용함으로써 쇄파현상에 대해서도 안정적인 수치해석을 할 수 있었다. 본 논문에서 개발된 수치방법을 적용한 문제는 다음과 같다. 첫째는 자유수면에서 실린더가 강제동요하는 경우에 자유표면형상과 힘을 계산하여 이전의 실험치 및 계산치와 비교하였다. 두번째로는 실린더가 자유수면하에서 일정한 속도로 항주하는 경우에 조파저항과 양력을 계산하여 고차 스펙트럴법과 비교하였다.

1. Introduction

When a body is doing the oscillation with large amplitude such as the slamming, the sloshing of fluid inside the tank and the ship overturning phenomenon in waves, etc., its solution is deviated from that of the linear analysis and a nonlinear analysis is required. Longuet-Higgins and Cokelet[1] who applied the complete nonlinear free surface condition to the analysis of the free surface flow for the first time, has calculated numerically a plunging

* 정회원, 현대중공업(주) 선박해양연구소

breaker problem by using comformal mapping in case that the depth of water is infinite. Since then, Faltinsen[2, 3] treated the sloshing problem inside a tank by using the method of source distribution, and the heaving problem of the two-dimensional floating body by using the Green's second identity. Vinje and Brevig[4] derived a boundary integral equation from Cauchy's theorem, and computed the heaving problem of foating body in waves by using the condition of periodicity as a matching condition. Dommermuth and Yue[5] treated heaving problem of an axisymmetric floating body by using the Green's second identity.

They used a solution of external field which obtained by numerical integration of the linear transient Green function to match with the nonlinear inner solution. The first problem treated in this paper is heaving and swaying motions of two dimensional floating body. Faltinsen[2], Vinje and Brevig[4] applied semi-Lagrangian-time stepping method to the problem of heaving motion of floating body. The second problem is the free surface problem generated by an submerged cylinder which runs with constant velocity. Havelock[6] computed wave resistance and lift force coefficients based on the linear theory for the case that submerged circular cylinder translates with constant velocity. Kim[7] obtained wave resistance for a submerged elliptic cylinder by using a higher order spectral method considering weakly nonlinear effect of free surface. This paper computes the free surface problems of submerged cylinders by applying fully nonlinear free surface conditions also using semi-Lagrangian time stepping method.

2. Formulation of boundary value problem

In the present work, we calculate two-dimensional initial boundary value problem by using both a complete free surface boundary condition and an accurate body surface boundary condition. Fluid is inviscid and incompressible, and velocity potential exists when fluid motion is assumed irrotational. In addition, surface tension is ignored and the depth of water is infinite. The present coordinate system(Fig. 1) is the space fixed coordinate system, keeping x-axis at a calm water and y-axis in vertical direction. The compuation domain is divided into the numerical calculation domain and the external domain where the linear free surface condition is applied. The total velocity potential Φ satisfies two dimensional Laplace equation as follows:

$$\nabla^2\Phi = 0 \quad ,t\geq 0 \tag{1}$$

The nonliear dynamic boundary condition of free surface is as follows:

$$\frac{D\Phi}{Dt} = \frac{1}{2} ww^* - gy \quad ,y=\eta(x) \tag{2}$$

where $w^* = u - iv$

The nonlinear kinematic boundary condition of free surface is as follows:

$$\frac{Dz}{Dt} = u + iv \quad ,y=\eta(x) \text{ where } z = x + iy \tag{3}$$

where u is the fluid velocity in x-direction, and v is that in y-direction. The boundary condition at body surface is as follows.

$$\Phi_n = V_n \quad ,t\geq 0 \tag{4}$$

where Φ_n is normal fluid velocity and V_n is normal velocity of body points. The equation of (4) is expressed as equation of (5) by transform[4].

$$\Psi = U_0(y-y_0) - V_0(x-x_0) - 1/2\,\dot{\theta}R^2 \tag{5}$$

where U_0 and V_0 are the body velocity at gravity center, and θ is the angle of rotation of body. Since the motion of body starts from rest,

initial condition is as follows:

$$\Phi = \frac{\partial \Phi}{\partial t} = 0. \qquad ,y \le 0 \ ,t < 0 \tag{6}$$

Linear velocity potential, ϕ, in external domain satisfies two-dimensional Laplace equation as follows.

$$\nabla^2 \phi = 0 \qquad ,t \ge 0 \tag{7}$$

Likewise, the linear boundary condition of free surface is as follows:

$$\frac{\partial \phi^2}{\partial t^2} + g\frac{\partial \phi}{\partial y} = 0 \qquad ,y = 0 \tag{8}$$

The boundary condition of the sea-bottom surface is as follows.

$$\frac{\partial \phi}{\partial y} = 0 \qquad ,y \to -\infty \tag{9}$$

The far field boundary condition is as follows.

$$|\nabla \phi| \to 0, \quad \text{at} \quad |z| \to \infty \tag{10}$$

The initial condition is as follows.

$$\phi = \frac{\partial \phi}{\partial t} = 0. \qquad ,y \le 0 \ ,t < 0 \tag{11}$$

3. Mathmatical formulation and the method of numerical computation.

3.1 The linear solution within external domain

The Green function is same as below when 2π is multiplied on both sides by using two-dimensional transient Green function of Wehausen and Laitone[8] and substituting $\delta(t-\tau)$ for source strength for numerical matching.

$$G(P,Q,t-\tau) = Re[\delta(t-\tau)\log(P-Q) + Re[\delta(t-\tau)\log(P-\overline{Q}) - 2gH(t-\tau)Re\int_0^\infty \frac{1}{\sqrt{gk}} e^{-ik(P-\overline{Q})}\sin[\sqrt{gk}(t-\tau))]dk \tag{12}$$

Green function G(P,Q,t-τ) is satisfied at boundary condition as same as in equation (8) ~ (11). It follows by using the Green's second identity for Green function and the property of the Delta function.

$$2\pi\phi(P,\tau) = \int_0^t d\tau \int_{\Sigma s} dS(\phi\frac{\partial G}{\partial n} - G\frac{\partial \phi}{\partial n}) \tag{13}$$

The velocity potential ϕ satisfies condition as follows on the matching surface.

$$\Phi = \phi, \quad \Phi_n = \phi_n \text{ on the matching surface} \tag{14}$$

The computation field is illustrated in Fig. 1.

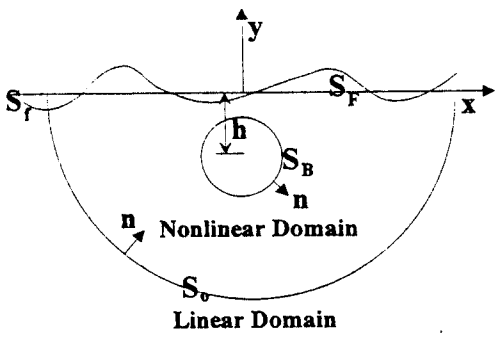

Fig. 1 Coordinate System and Domain Definition

When integration by part is executed for τ by using the free surface boundary condition and far field boundary condition about the Green function in equation (13). The equation of (13) is expressed as follows.

$$2\pi\phi(P,\tau) = \int_0^t d\tau \int_{S_0} dS(\phi\frac{\partial G}{\partial n} - G\frac{\partial \phi}{\partial n}) \tag{15}$$

The equation of (15) should be substituted for matching with the Cauchy's theorem in the nonlinear domain. The Cauchy-Riemann relation is as follows.

$$\frac{\partial \phi}{\partial n} = -\frac{\partial \psi}{\partial s} \tag{16}$$

It is as follows when the second term is done integration by part for s by substituting (16) in (15)

$$2\pi\phi(P,\tau)=\int_0^t d\tau\int_{S_0} dS(\phi\frac{\partial G}{\partial n}-\psi\frac{\partial G}{\partial s})+\int_0^t d\tau\,[G\psi]^{s1}_{s2} \tag{17}$$

s1 and s2 are intersection point of a matching boundary and a free surface in (17). The first term on the right hand side in (17) is the form of space integral and time integral about normal dipole and tangential dipole on the matching boundary, and the second term in s1, s2 is the form of time integral about point source. First of all, G is divided G_R of the singular part into Gw which is discribing the memory effect of free surface, and let (12) substitute into (17), then it is possible to get the matching matrix. The segment of dS is discritized as line element and the time integrations of ϕ and ψ make use of the simpson rule. The line integrals with the first and second term in relation to equation (12) are expressed as follows in (17).

$$\int_{S_j}\frac{\partial G_R}{\partial n}dS=[\tan^{-1}\frac{(\eta-y)}{(\xi-x)}-\tan^{-1}\frac{(\eta+y)}{(\xi-x)}]^{j+1}_j \tag{18}$$

$$\int_{S_j}\frac{\partial G_R}{\partial s}dS=\mathrm{Re}[\log(Q-P)]^{j+1}_j+\mathrm{Re}[\log(\overline{Q}-P)]^{j+1}_j \tag{19}$$

The first term of (18) get π value when i equal to j. It is well known that Gw of (12) is expressed by the Error function[9].

$$G_W=\mathrm{Re}[-2g\int_0^\infty dk\,e^{-i(P-\overline{Q})}\sin[\sqrt{gk}(t-\tau))]]=\frac{4\pi}{t-\tau}Xe^{X^2}\mathrm{erf}(X)$$

$$X^2=\frac{ig(t-\tau)^2}{4(P-Q)} \tag{20}$$

For the moment, let the harmonic Green function of (12) in relation to Gw represent f = f_R + if_I. When the Cauchy-Riemann relation is used, the integral calculation regarded of Gw of (17) is same as below.

$$\int_{S_j}\frac{\partial G_W}{\partial n}dS=\int_{S_j}\frac{\partial f_R}{\partial n}dS=-\int_{S_j}df_I=f_I(P,\overline{Q_j},t-\tau)-f_I(P,\overline{Q_{j+1}},\tau) \tag{21}$$

$$\int_{S_j}\frac{\partial G_W}{\partial s}dS=\int_{S_j}\frac{\partial f_R}{\partial s}dS=-\int_{S_j}df_R=f_R(P,\overline{Q_{j+1}},t-\tau)-f_R(P,\overline{Q_j},\tau) \tag{22}$$

The Error function is expressed by using ascending series and asymtotic expansions [10]. Resultly, the time integral calculation is executed as follows.

Ascending series($X\ll 1$)

$$\int_{t_n}^{t_{n+1}}d\tau\frac{4\pi}{t-\tau}Xe^{X^2}\mathrm{erf}(X)=8\sum_{n=0}^{\infty}\frac{2^nX^{2n+1}}{1\cdot3\cdot5\cdot\cdots(2n+1)} \tag{23}$$

Asymtotic expansion($X\gg 1$)

$$Xe^{X^2}\mathrm{erf}(X)=\frac{1}{\pi}\sum_{m=0}^{\infty}\frac{(-1)^m1\cdot3\cdot5\cdot\cdots(2m-1)}{(2X)^m},\quad \arg(X)<\frac{3\pi}{4} \tag{24}$$

$$\int_{t_n}^{t_{n+1}}d\tau\frac{4\pi}{t-\tau}Xe^{X^2}\mathrm{erf}(X)=\frac{-2\pi}{X}[1+\sum_{m=0}^{\infty}\frac{(-1)^m1\cdot3\cdot5\cdot\cdots(2m-1)}{(2X)^m}]+4[\log X+\sum_{m=1}^{\infty}\frac{(-1)^{m-1}1\cdot3\cdot5\cdot\cdots(2m-1)}{2m(2X)^m}],\ -\frac{3\pi}{4}<\arg(X)<\frac{\pi}{4} \tag{25}$$

$$=\frac{2\pi}{X}[1+\sum_{m=0}^{\infty}\frac{(-1)^m1\cdot3\cdot5\cdot\cdots(2m-1)}{(2X)^m}]+4[\log X+\sum_{m=1}^{\infty}\frac{(-1)^{m+1}1\cdot3\cdot5\cdot\cdots(2m-1)}{2m(2X)^m}],\quad \frac{\pi}{4}<\arg(X)<\frac{5\pi}{4} \tag{26}$$

3.2 The solution of nonlinear doamin

In order to give an account of motion of fluid, the complex potential which is made by $\beta(z,t)=\Phi(x,y,t)+\Psi(x,y,t)$ is introduced.

$\Phi(x,y,t)$, $\Psi(x,y,t)$ are satisfied by The Cauchy-Riemann relation in fluid field so that is analytical. Hence, it is possible to apply the Cauchy's theorem.

$$\oint_C\frac{\beta(z;t)}{(z-z_0)}dz=0 \tag{27}$$

z_0 is in the outside of closed boundary C within fluid. C is consisted of the free surface, body surface and matching surface. From time integral (2), Φ is known in the free surface boundary side(C_ϕ), and (5), Ψ is kown in the

solid boundary side(C_Ψ). The relative equation of Φ and Ψ is given in the matching boundary side(C_Φ or C_Ψ). When (27) is taken a real and imaginary part with z_0 of C, it is possible to get the Fredholm second integral equation as follows.

$$a\Psi(x_0, y_0; t) + \mathrm{Re}\left[\int_C \frac{\Phi + i\Psi}{z - z_0} dz\right] = 0 \quad \text{, for } z_0 \text{ on } C_\Phi \tag{28}$$

$$a\Phi(x_0, y_0; t) + \mathrm{Im}\left[i\int_C \frac{\Phi + i\Psi}{z - z_0} dz\right] = 0 \quad \text{, for } z_0 \text{ on } C_\Psi \tag{29}$$

a is solid angle between two tangent line, z_0 to C. In order to slove unkown values, Φ and Ψ, let those divide into z_k about integral boundary(C), and Φ and Ψ assume the linear variation of complex potential on line segment. Concerning about the progress of matrix calculation, Chapter 3.3 gives help for reference. For the computation of the next time step, a body surface position, a fluid particle position on the free surface and a velocity potential shoud be decided. The position of body surface is given by solving the equation of motion, or is able to know from forced motion mode, and the stream function is given from (5), and the position of fluid particle and the velocity potential of the free surface are obtained by time integration from (2) and (3). For the time integration of (2) and (3), the initial four steps make use of the method of fourth-order Runge Kutta, and the time steps after those make use of the method of Hamming's fourth-order predicted/corrector. The velocity computation of a fluid particle on the free surface is obtained as the concept by the centeral difference.

3.3 Matrix Computation of the Linear and Nonlinar Solution

Φ is unkown on a body surface in the nonlinar domain, Ψ is unkown on a free surface and Φ, Ψ are both unkown on the matching boundary. When Φ is substituted (27) by making relative formula of Φ and Ψ in (17), Ψ is unkown. The matching condition is same as (14) on a matching boundary. It is as follows when (15) is expressed as matrix form by applying (14).

$$\begin{aligned} |\Phi| &= |A|^{-1}|B||\Psi| + |A|^{-1}|C_1|\Psi_{S2+} + |A|^{-1}|C_2|\Psi_{S1+} + |A|^{-1}|C| \\ &= |a||\Psi| + |c_1|\Psi_{M+1} + |c_2|\Psi_{N2} + |d| \end{aligned} \tag{30}$$

N1+1 and N2 are element numbers of intersection point on the free surface and matching surface. The equation of (30) is relation of velocity potential and stream function, and the linear free surface boundary condition is satisfied on a matching surface. When (28) and (29) are discritized as line segments, the matrix forms are shown as follows.

$$\mathrm{Re}\left[\int_C \frac{\Phi + i\Psi}{z - z_0} dz\right] = \mathrm{Re}\left[\sum_{j=0}^{N3} \Gamma_{k,j}(\Phi_j + i\Psi_j)\right] = 0, \quad \text{for } z_k \text{ on } C_\Phi \tag{31}$$

$$\mathrm{Re}\left[i\left[\int_C \frac{\Phi + i\Psi}{z - z_0} dz\right]\right] = \mathrm{Re}\left[i\sum_{j=0}^{N3} \Gamma_{k,j}(\Phi_j + i\Psi_j)\right] = 0 \quad \text{for } z_k \text{ on } C \tag{32}$$

N3 is total element number and correlation function , $\Gamma_{k,j}$, is as follows.

$$\Gamma_{k,j} = \frac{z_k - z_{j-1}}{z_j - z_{j-1}} \log\frac{z_j - z_k}{z_{j-1} - z_k} + \frac{z_k - z_{j+1}}{z_j - z_{j+1}} \log\frac{z_{j+1} - z}{z_j - z_k} \tag{33}$$

The matrix equation with the linear domain is derived by using (30) of the matching condition according to boundary. It is as follows when replacing (30) with (31) and (32).

$$\begin{aligned} &(-\mathrm{Im}\Gamma_{k,1} + \mathrm{Re}\Gamma_{k,1}a_{1,1} + \mathrm{Re}\Gamma_{k,2}a_{2,1} + \cdots + \mathrm{Re}\Gamma_{k,N1+1}a_{N1,1})\Psi_1 + \\ &(-\mathrm{Im}\Gamma_{k,2} + \mathrm{Re}\Gamma_{k,1}a_{1,2} + \mathrm{Re}\Gamma_{k,2}a_{2,2} + \cdots + \mathrm{Re}\Gamma_{k,N1+1}a_{N1,2})\Psi_2 + \\ &\quad\vdots \\ &(-\mathrm{Im}\Gamma_{k,N1} + \mathrm{Re}\Gamma_{k,1}a_{1,N1} + \mathrm{Re}\Gamma_{k,2}a_{2,N1} + \cdots + \mathrm{Re}\Gamma_{k,N1+1}a_{N1,N1})\Psi_{N1} + \\ &\sum_{j=1}^{N2}(\mathrm{Re}\Gamma_{k,j}c_{2j,N2} - \mathrm{Im}\Gamma_{k,N2})\Psi_{N2} + \sum_{j=1}^{N3}(\mathrm{Re}\Gamma_{k,j}c_{1j,M+1} - \mathrm{Im}\Gamma_{k,M+1})\Psi_{M+1} - \\ &\sum_{j=M+2}^{N2-1}\mathrm{Im}\Gamma_{k,j}\Psi_j + \sum_{j=N2+1}^{N3}\mathrm{Re}\Gamma_{k,j}\Phi_j = -\sum_{j=M+1}^{N2}\mathrm{Re}\Gamma_{k,j}\Phi_j + \sum_{j=N2+1}^{N3}\mathrm{Im}\Gamma_{k,j}\Psi_j \\ &\quad - \sum_{j=1}^{N3}\mathrm{Re}\Gamma_{k,j}d_j \end{aligned}$$

where z_k is on C_ϕ (34)

$$(-\mathrm{Re}\Gamma_{k,1}-\mathrm{Im}\Gamma_{k,1}a_{1,1}-\mathrm{Im}\Gamma_{k,2}a_{2,1}+\cdots-\mathrm{Im}\Gamma_{k,N1+1}a_{N1,1})\Psi_1+$$
$$(-\mathrm{Re}\Gamma_{k,2}-\mathrm{Im}\Gamma_{k,1}a_{1,2}-\mathrm{Im}\Gamma_{k,2}a_{2,2}+\cdots-\mathrm{Im}\Gamma_{k,N1+1}a_{N1,2})\Psi_2+$$
$$\vdots$$
$$(-\mathrm{Re}\Gamma_{k,N1}-\mathrm{Im}\Gamma_{k,1}a_{1,N1}-\mathrm{Im}\Gamma_{k,2}a_{2,N1}+\cdots-\mathrm{Im}\Gamma_{k,N1+1}a_{N1,N1})\Psi_{N1}+$$
$$(\sum_{j=1}^{N2}-Im\Gamma_{k,j}c_{2j,N2}-Re\Gamma_{k,N2})\Psi_{N2}+(\sum_{j=1}^{N1}-Im\Gamma_{k,j}c_{1j,N1+1}-Re\Gamma_{k,N1+1})\Psi_{N1+1}-$$
$$\sum_{j=N1+2}^{N2-1}Re\Gamma_{k,j}\Psi_j-\sum_{j=N2+1}^{N2}Im\Gamma_{k,j}\Phi_j=\sum_{j=N1+1}^{N2}Im\Gamma_{k,j}\Phi_j+\sum_{j=N2+1}^{N1}Re\Gamma_{k,j}\Psi_j$$
$$+\sum_{j=1}^{N1}Im\Gamma_{k,j}d_j$$

where z_k is on C_ψ (35)

3.4 Hydrodynamic Force and Moment

When $\frac{\partial\phi}{\partial t}$ is substituded in the Green's second identity instead of ϕ, the equation of (17) is possible to replace as follows, as it is satisfied with (7) ~ (11) in the linear field.

$$2\pi\phi_t(P,t)=\int_0^t d\tau\int_{S_B}dS(\phi_t\frac{\partial G}{\partial n}-\psi_t\frac{\partial G}{\partial s})+\int_0^t d\tau\,[G\psi_t]^{s1}_{s2} \tag{36}$$

$\beta_t(z,t)=\Phi_t(x,y,t)+\Psi_t(x,y,t)$ is the harmonic function in the linear field, so that it is as follows by using the Cauchy's theorem.

$$\oint_C\frac{\beta_t(z;t)}{(z-z_0)}dz=0 \tag{37}$$

In equation (36), when ϕ_t is substituded in (37), the matrixs of the same form (34) and (35) are deduced. In matrix equations which are equal (34) and (35), let ϕ_t and ψ_t convert instead of Φ and Ψ. ϕ_t is unkown on a body surface, ψ_t is unkown on a free surface, and ϕ_t and ψ_t are unkown on the matching surface. The boundary conditions in ϕ_t and ψ_t to obtain hydrodynamic force are as follows.

$$\frac{\partial\Phi}{\partial t}=(y-y_0)a_{x_0}-(x-x_0)a_{y_0}-\frac{1}{2}R^2\theta+u_0v-v_0u$$
$$+[(u_0-u)(x-x_0)+(v_0-v)(y-y_0)]\theta\ ,$$

on the body boundary (38)

$$\frac{\partial\Phi}{\partial t}=\frac{1}{2}ww^*-gy\ ,\text{on the free surface} \tag{39}$$

$$[\Phi_t]=[\phi_t],\quad[\Psi_t]=[\phi_t]\ ,$$

on the matching boundary (40)

By using (38) ~ (40), when (36) is compared with (17), left hand side matrix is not changed, only right hand side matrix is changed. It is possible to get ϕ_t by solving the matrix once more. The hydrodynamic force and moment is obtained from the Bernoulli equation.

$$F=-\int_{S_B}p\cdot n\,dS=i\rho\int_{S_B}[-\frac{\partial\Phi}{\partial t}+\frac{1}{2}ww^*]n_x dS+ \tag{41}$$
$$j\rho\int_{S_B}[-\frac{\partial\Phi}{\partial t}+\frac{1}{2}ww^*]n_y dS$$

$$F=-\int_{S_B}p[-(y-y_G)n_x i+(x-x_G)n_y j]\,dS=-i\rho\int_{S_B}[-\frac{\partial\Phi}{\partial t}+\frac{1}{2}ww^*]$$
$$(y-y_G)n_x dS+j\rho\int_{S_B}[-\frac{\partial\Phi}{\partial t}+\frac{1}{2}ww^*](x-x_G)n_y dS$$

(42)

4. The Simple Harmonic Forced-Oscillation

4.1 Calculation of Submerged Circular Cylinder

The hydrodynamic force on a cylinder is computed when a submerged circular cylinder does the forced harmonic motion. It is in case that the body moves by mode of y=-Acos(wt), and the hydrostatic force by static pressure is ignored in this computation. As computation example, there is a submerged circular cylinder which does heave or sway oscillation. It is the case that nondimensional wave frequency $K_R(=w^2R/g)$ is 1, and the distance from center of cylinder to a matching boundary is 2.3 times of wave length. The numbers of element in one wave length are 26 and it does time progress for 5 periods. Fig. 2 shows the wave form of the case of K_R=1, h/R=1.3, A_3/R=0.25. When observing the waves precisely, The nonlinear wave is occurred near a circular cylinder. This

method is possible to do stable numerical analysis, and the waves almost does not reflect although the waves reach on the matching boundary. The computation is impossible to be progressed if the regridding technique does not use. Fig. 3 is the case of K_R=1, h/R=1.3, A_3/R=0.1, 0.25.

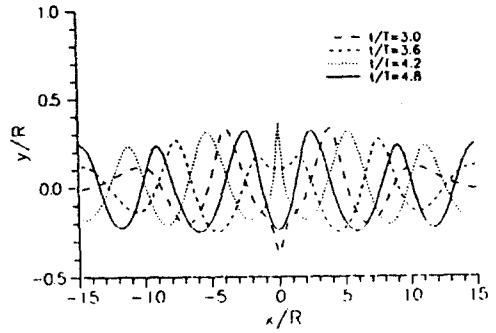

Fig. 2 Wave Profile Generated by Heaving Circular Cylinder under Free Surface (K_R=1, h/R=1.3, A_3/R=0.25)

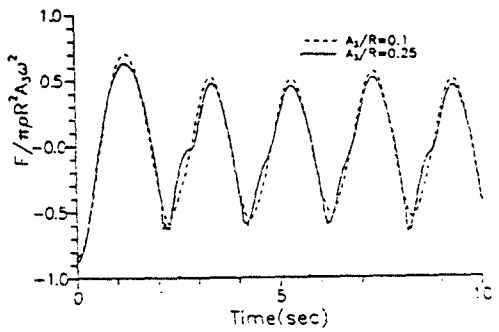

Fig. 3 Time History Forces for Heaving Circular Cylinder under Free Surface(K_R=1, h/R=1.3)

Fig. 4 is a computation of K_R=1, h/R=2., A_3/R=2. in case that the submerged circular cylinder does sway oscillation, it shows the configuration that the wave after 3 period is breaking, and the computation is broken when breaking and over turning waves reach the matching boundray. Fig. 5 shows the hydrodynamic forces in case of K_R=1, h/R=2., A_3/R=0.4, 2. In case of sway oscillation, it shows that a nonlinear hydrodynamic force is smaller than the case of heave oscillation and the force of y-direction is shown. The period of y-directional force is about 1/2 of that of x-directional force, the reason is due to a effect of velocity square term in the Bernoulli equation.

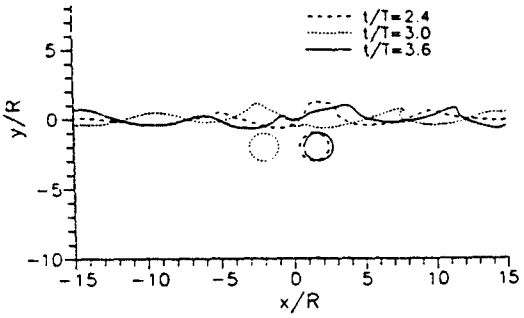

Fig. 4 Wave Profile Generated by Swaying Circular Cylinder under Free Surface (K_R=1, h/R=2, A_3/R=2)

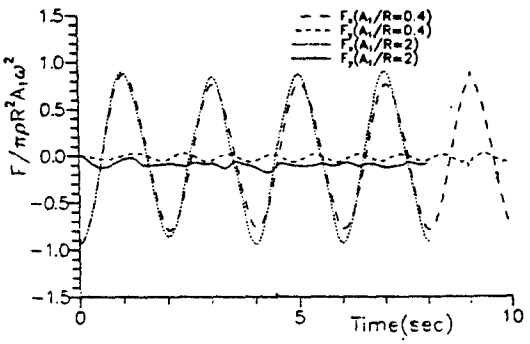

Fig. 5 Time History Forces for Swaying Circular Cylinder under Free Surface(K_R=1, h/R=2)

4.2 Calculation of Foating Circular Cylinder

The wave profile and hydrodynamic force are computed when a circular cylinder does forced harmonic motion. The time integrations are proceeding to six periods on the case that a circular cylinder moves mode of y=Asin(wt), and the distance from center of cylinder to the matching boundary is 3.18 times of wave length. The numbers of mesh per one wave are 25. The

computation of a heaving or swaying cylinder is executed as changing nondimensionalized wave frequency and the ratio of amplitude. Fig. 6 compares the results concerning about the K_R=1, A_3/R=0.1 with the results of Faltinsen[2]. It shows that a result of computation of the initial moment accords with the result of Faltinsen comparatively. In order to examine the effect by the matching boudary, Fig. 7 compares the hydrodynamic force about distance effect from center of the rectangular cylinder to the matching boundary(=2.86, 3.5). As a result, it is estimated that the matching is working well in case that matching length is long. Because it is matching with linear solution, it is impossible to be a exact matching when nonlinear waves reach on the matching side.

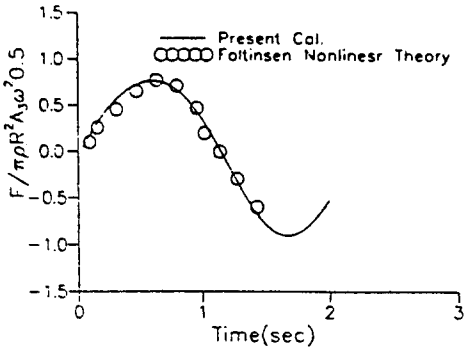

Fig. 6 Time History Force for Heaving Circular Cylinder (K_R=1, A_3/R=0.1)

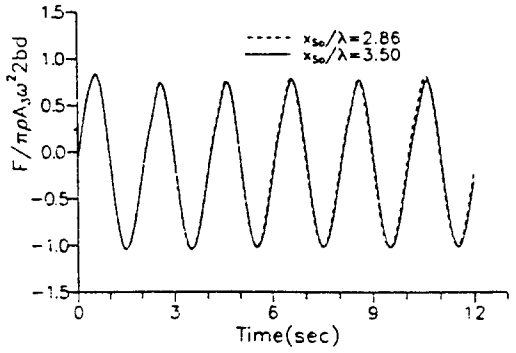

Fig. 7 Time History Force for Heaving Rectangular Cylinder (K_R=1, A_3/R=0.1)

Fig. 8 shows the wave form in case of the ratio of amplitude is 0.6 and Fig. 9 shows hydrodynamic force in case that amplitude is 0.1, 0.4 and 0.6. When the ratio of motion amplitude is getting large, nonlinear effect in equilibrium position is especially getting large, and the nonlinear effect in the initial transient state is prominant.

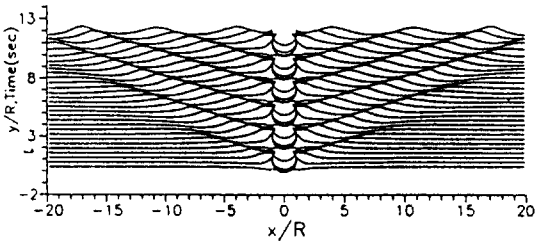

Fig. 8 Wave Profile Generated by Heaving Circular Cylinder (K_R=1, A_3/R=0.6)

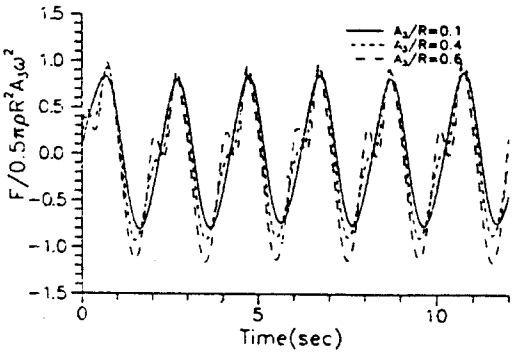

Fig. 9 Time History Force for Heaving Circular Cylinder (K_R=1)

When the hydrodynamic forces are done Fourier transformation, it is possible to obtain the time mean force component, first harmonic force component and second harmonic force component. If the motions reach in the steady state, it should compute more than three periods at least. As a uncertainty of solution by the linear matching is considered, The Fourier transform is chosen by the fifth period of

hydrodynamic force. It is compared the component of hydrodynamic force from these procedure, with the result of Ursell[11], and the experimental value of Yamashita. Fig. 10 is a figure about the added mass when the number of wave are changing. it is getting a little larger than the result of Ursell, and the value of A_3/R=0.4 is larger than that of A_3/R=0.2. In Fig. 11, the damping coefficeint has a difference with the result of Ursell when the ratio of amplitude is getting large. Resultly, the nonlinearity by motion is getting large. Fig. 12 shows the time mean force coefficient. It accords with the result of Ursell. Fig. 13 is amplitude of the second harmonic force component, it also accords with the result of Ursell. The value is a little larger A_3/R=0.2 than the case of A_3/R=0.4. Generally, the present calculation are accorded with the experiment.

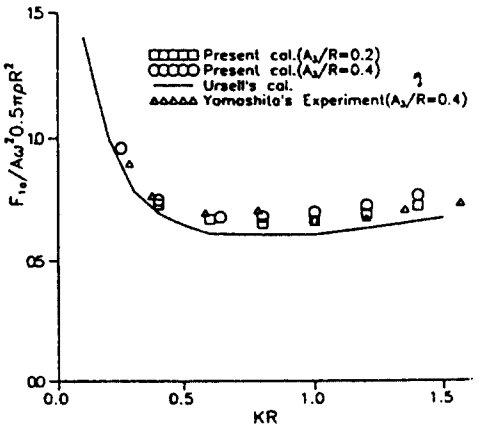

Fig. 10 Heave Added Mass Coefficient of Floating Circular Cylinder

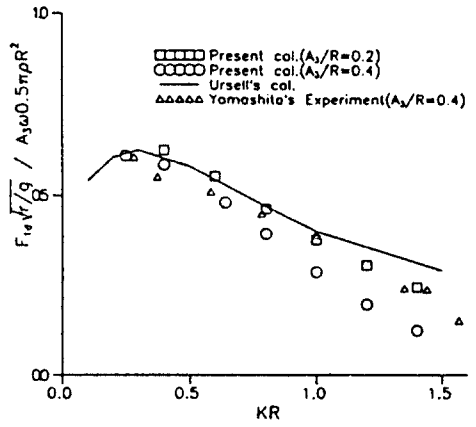

Fig. 11 Heave Damping Coefficient of Floating Circular Cylinder

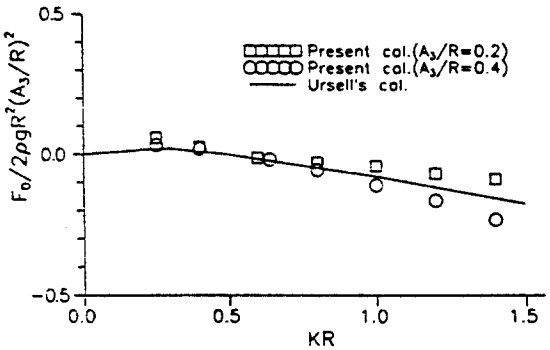

Fig. 12 Heave Time Mean Force Coefficient of Floating Circular Cylinder

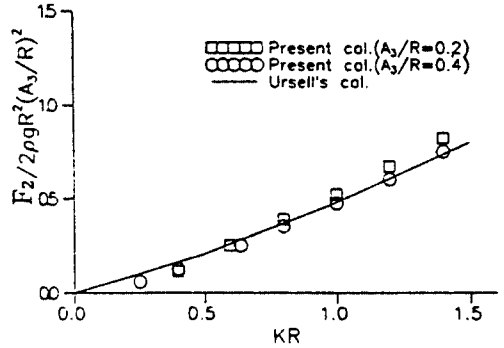

Fig. 13 Heave 2nd Harmonic force Coefficient of Floating Circular Cylinder

Concerning of the computation of swaying circular cylinder, it computes hydrodynamic force and wave profile according to wave frequency. When the linear free surface condition is imposed in itersection point of free surface and body surface, it has difficulty to have logarithm singularity. In this computation, the position of intersection point is extrapolated from free

surface in order to process numerically, and the boundary condition from the body surface is adopted. As a result, the computation is very well proceeded. Fig. 14 shows the wave profile about K_R=1, A_3/R=0.4. Fig. 15 shows the hydrodynamic force this case, hydrodynamic force is quite decreased in 6 periods, the reason is the increase of errors which caused by intersection point not satisfied the mass conservation and the matching of the linear domain gives effect to numerical solution of the internal domain. Fig. 16 is hydrodynamic force in case of K_R=0.4, A_3/R=0.4. it also computes y-directional force. When the ratio of amplitude and wave frequency are decreased, a y-directional force is decreased, and a period is always 1/2 of oscillation period. Fig. 17 shows the added mass coefficient and damping coefficient, the added mass is increased when wave frequency are decreased, and it has a difference with the result of Frank[12] when it is increased. The damping coefficient has a result that the maximun value is a little difference with the result of Frank.

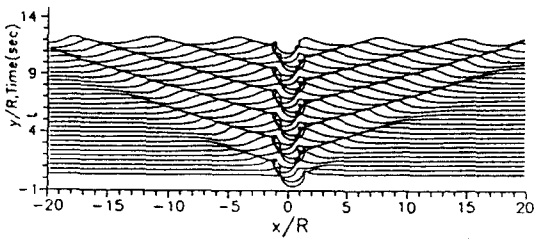

Fig. 14 Wave Profile Generated by Swaying Circular Cylinder (K_R=1, A_3/R=0.4)

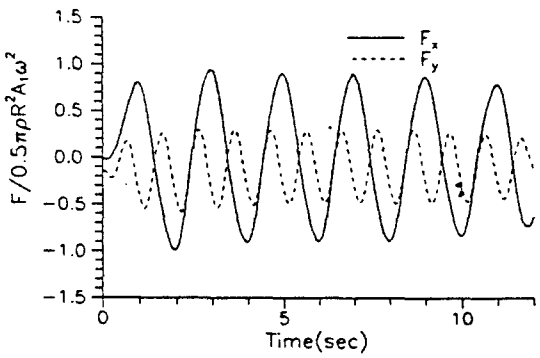

Fig. 15 Time History Force for Swaying Circular Cylinder (K_R=1, A_3/R=0.4)

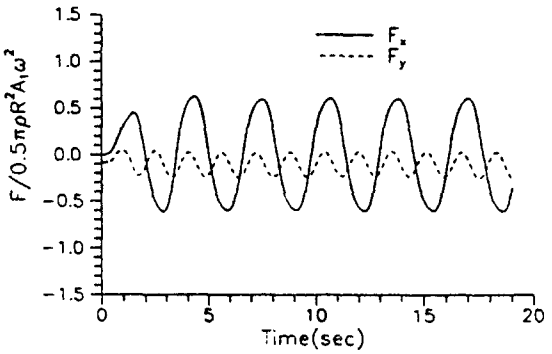

Fig. 16 Time History Force for Swaying Circular Cylinder (K_R=0.4, A_3/R=0.5)

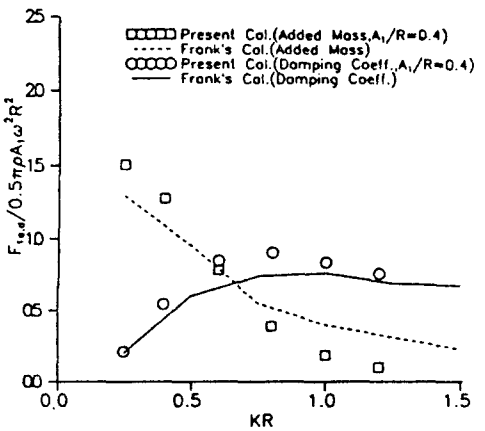

Fig. 17 Sway Added Mass and Damping Coefficient of Floating Circular Cylinder

5. Uniformly Translating Cylinder

As the example of computation, it is in case that the circular cylinder and elliptic cylinder advance horizontally with constant velocity starting from rest. In advance, a circular cylinder which is example of Havelock[6] let translate with the following velocity.

$$U(t)=0 \quad ,t<0 \qquad (43)$$
$$=-U_0 \ , \ t\geq($$

Fig. 18 is the computation of the wave profile in case that R is 1. The submerged depth h is 2 and the Froude number about depth is F_h=0.6. Fig. 18 shows the configuration that wave is breaking. It is seen from Fig. 18 that Havelock does a computation under linear assumption, or it is the effect of transient wave by suddern acceleration in t=0. As a result, it let the circular cylinder by the velocity distribution as follows accelerate from t=0 slowly.

$$U(t)=-\frac{U_0}{2}[1-\cos(\pi t/Tacc)] \ ,t<Tacc \qquad (44)$$
$$=-U_0 \ , \ t\geq Tacc$$

Let Fig. 19 accelerate to Tacc=10 sec with the same velocity as (44). In this moment, the waves are breaking, and the computation is broken down about t=9.2 sec like the same case Fig. 18. The reason why the waves are breaking is not because of transient wave, but because the model of computation has strong nonlinearity. For the evidence, when the wave profile is observed in F_h=0.6 in the linear computation of Kim[13], the ratio wave height and length is about 0.35. This proves that present computation is right because the wave steepness beyond 1/7 makes wave unstable. This shows that physical phenomenon is not aware by the linear asumption of the free surface.

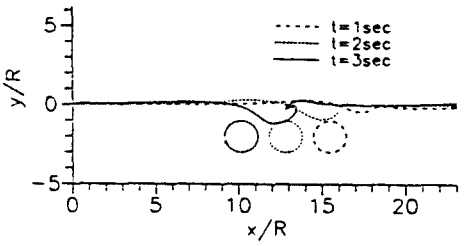

Fig. 18 Wave Profile Generated by Uniformly Translating Circular Cylinder(Impulsive Start, F_h=0.6, h/R=2)

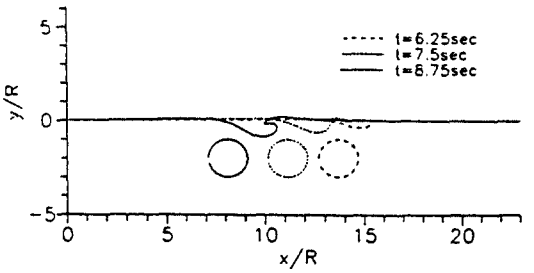

Fig. 19 Wave Profile Generated by Uniformly Translating Circular Cylinder(Smooth Start, F_h=0.6, h/R=2, Tacc=10 sec)

For the purpose of decreasing the nonlinearity of the free surface by the cylinder, the elliptic cylinder adopted as calculation model. It compares with the higher order spectral method as changing submerged depth about the Froude number (FL=0.70117). In advance, it makes impulsive start such as (43) in case that it is FL=0.70117, h/L=2. Fig. 20 and Fig.21 show the wave profile, wave-making resistance and lift by waves. The transient phenomenon of hydro-dynamic forces by abrupt start of initial state is continued, and the shapes of wave also show irregular phenomenon. In order to deviate transient phenomenon, the smooth start like (44) is required. Fig.22 and Fig.23 show the wave profile, wave-making resistance and lift by waves(FL=0.70117, h/L=2). The wave-making resistance has a little small value comparing with the higher order spetral method, and the lift gives large values. Fig.24 and Fig.25 show the wave profile, wave-making resistance and lift in FL=0.70117, h/L=1.7. The shapes of wave are accorded with Ogiwara's[14] experimental value and the values of resistance are also accorded with the spectral method, however, the lift has present calculation differ a value of the spectral method. When synthesizing the results, the wave-making resistance and lift value are oscillating at mean value even though reaching

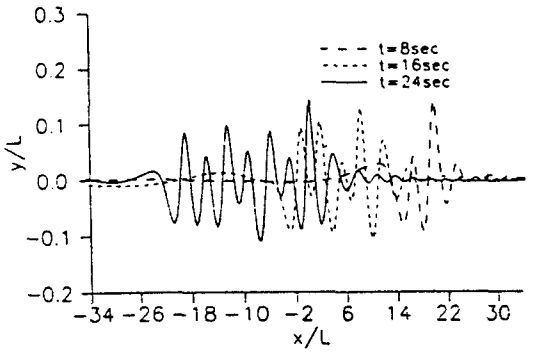

Fig. 20 Wave Profile Generated by Uniformly Translating Elliptic Cylinder(Impulsive Start, F_L=0.70711, h/L=2, b/L=0.25)

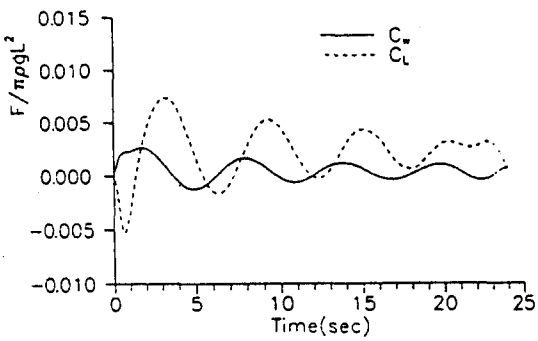

Fig. 21 Time History Forces by Uniformly Translating Elliptic Cylinder(Impulsive Start, F_L=0.70711, h/L=2, b/L=0.25)

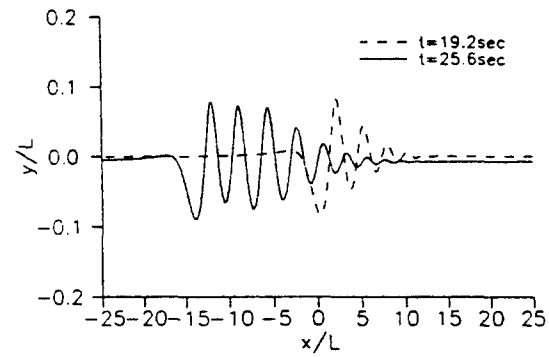

Fig. 22 Wave Profile Generated by Uniformly Translating Elliptic Cylinder(Smooth Start, FL=0.70711, h/L=2, b/L=0.25, Tacc=18sec)

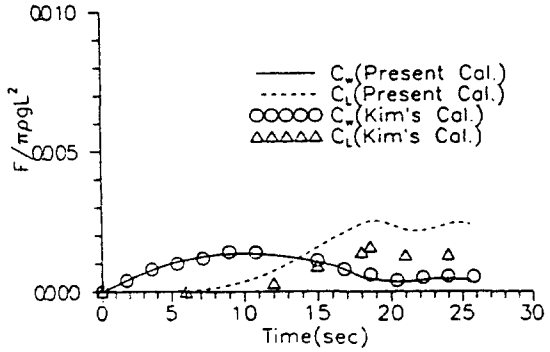

Fig. 23 Time History Forces by Uniformly Translating Elliptic Cylinder(Smooth Start, F_L=0.70711, h/L=2, b/L=0.25, Tacc=18sec)

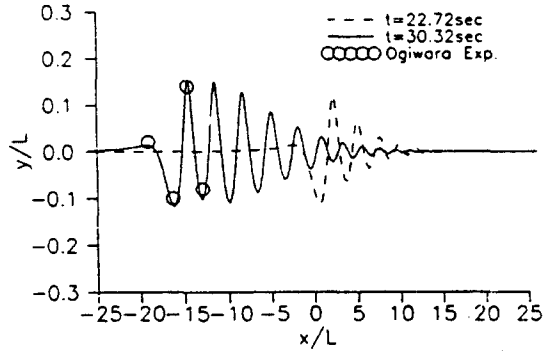

Fig. 24 Wave Profile Generated by Uniformly Translating Elliptic Cylinder(Smooth Start, F_L=0.70711, h/L=1.7, b/L=0.25, Tacc=24sec)

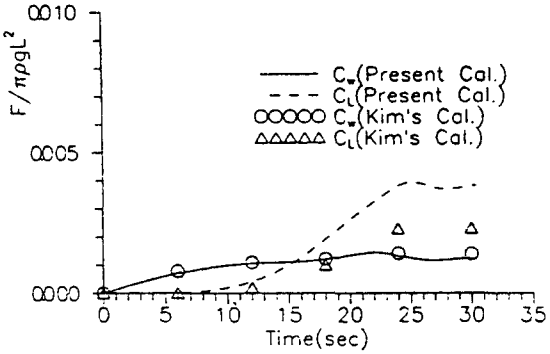

Fig. 25 Time History Forces by Uniformly Translating Elliptic Cylinder(Smooth Start, F_L=0.70711, h/L=1.7, b/L=0.25, Tacc=24sec)

steady state. The reason is that the computation in time domain is differ from the computation in frequency domain - the shape of wave behind the body is fluctuated, and the oscillating period is same as the period that wave is formed.

6. Conclusion

This paper develops a numerical method in time domain to analyize two dimensional nonlinear motion. The field of computation is divided into the internal field near body where the nonlinear free surface boundary condition and body boundary condition are satisfied strictly and the external field where the linear free surface boundary condition and radiation condition are satisfied. The solution of internal field is obtained by using the Cauchy's boundary integral equation, and the Green's second identity including the transient Green function is used to obtain the solution of the external field. The matrix equations which come from two fields above are connected into one matrix equation applying the matching condition. For the purpose of validation of computing results, we compare the present compuation values with other theoretical and experimental results. Though this research, the following conclusions are obtained.

1) In case of heaving oscillation of floating circular cylinder, the damping coefficient agrees with the computation value of Ursell but it has a large difference in high frequency range. The present calculation result of added mass is a little larger than that of Ursell. However, it agrees with the experiment value. The time mean force and second harmonic force show good agreement with the calculation-value of Ursell and the experiment-value of Yamashita.

2) The cross product force in vertical direction of swaying cylinder is due to the velocity square term which is nonlinear term of the Bernoulli equation.

3) In case that a submerged elliptic cylinder abruptly starts, the transient effect is maintained for a long time. As a result, long simulation time is required to obtain the steady solution but in case of smooth start the steady solution is stably obtained within relatively short simulation time. In case of advancing submerged circular cylinder, the breaking and over-turning waves are generated when the Froude number is 0.6, 0.8 and 1.

References

1) Longuet-Higgins,M.S. and Cokelet,E.D.,"The Deformation of Steep Surface Waves on Water :I.A Numerical Method of Computation", Proc. Soc. London A.350, 1976.

2) Faltinsen, O.M., "Numerical Solution of Transient Nonlinear Free-Surface Motion Outsider Inside Moving Bodies",Proc. 2nd Int. Conf. on Num. Ship Hydrodyn.,1977

3) Faltinsen, O.M.,"Numerical Nonlinear Method of Sloshing in Tanks with Two-Dimensional Flow", J. of Ship Res., Vol.22, No.3, 1978.

4) Vinje,T. and Brevig, P.,"Nonlinear Ship Motion", Proc. 3rd Int. on Num. Ship Hydrodyn., 1981.

5) Dommermuth,D.G. and Yue,D.K.,"Numerical Simulations of Nonlinear Axisymmetric Flows with Free Surface", J. of Fluid Mech., Vol.178,1987.

6) Havelock,T.H.,"The Forces on a Circular Cylinder Submerged in a Uniform Stream", the Collected Papers of Sir Thomas Havelock on Hydrodynamics, 1936.

7) Kim,Y.J. and Hwang,J.H.,"A Study on the Development of 2-Dimensional Numerical Wave Tank by the Higher-Order Spectral Method", J. of SNAK, Vo.29, No.3, 1992.

8) Wehausen,J.V. and Laitone,E.V.,"Surface Waves", Encyclopedia of Physics, Vol.9 Springer-Verlag, 1960.
9) Abramowitz, M. and I.A. Stegun,"Handbook of Mathematical Function", Dover Publication, 1965
10) Gradshteyn,I.S. and Ryzhik,I.M.,"Table of Integrals, Series and Products", Academic Press, 1980.
11) Ursell,F.,"On the Heaving Motion of a Circular Cylinder on the Surface of a Fluid", Quarterly J. of Mech. and Appl. Math., Vol.2, 1949.
12) Frank,W.,"Oscillation of Cylinders in or below the Free Surface of Deep Fluids", NSRDC Report 2375, 1967.
13) Kim,Y.J. and Hwang,J.H.,"The Two Dimensional Transient Motions with Large-Amplitude by Time domain Analysis", Proc. 16th ONR Symp., 1986.
14) Ogiwara, S.,"A Numerical Method of Nonlinear Solution for Steady Waves Induced by Two-Dimensional Submerged Bodies", J. of SNAJ ,Vol.156, 1974.